applied sciences

MDPI

Article

Dynamic Behaviour of an Automotive Dual Clutch Transmission during Gear Shift Maneuvers

Renato Brancati *,†, Stefano Pagano † and **Ernesto Rocca †**

Dipartimento di Ingegneria Industriale, Università di Napoli Federico II, Via Claudio 21, 80125 Napoli, Italy; stefano.pagano@unina.it (S.P.); erocca@unina.it (E.R.)

* Correspondence: renato.brancati@unina.it

† These authors contributed equally to this work.

Abstract: The paper presents a model for the torsional dynamics of an automotive driveline equipped with a Dual Clutch Transmission (DCT), focusing on the gear rattle phenomenon arising during the transients of engagement and disengagement of the clutches, and during the synchronizing manoeuvres. This vibro-acoustic phenomenon, particularly annoying in automotive transmissions, can be accentuated by the presence of many unloaded gears in this type of gearbox. Dual Clutch Transmission systems are today largely diffused in the car automatic transmissions, permitting fast gear shifts and avoiding the interruption of the drive torque. The study is conducted by adopting a tribo-dynamic model with lumped parameters, considering the oil lubricant between the teeth of the unloaded gears acting as a damper during the impacts. A layout of a gearbox with six speed ratios has been assumed, in which a dual clutch system transmits the drive torque alternatively between the various gear pairs in the odd and even branches. The results of the numerical simulations show that this kind of transmission system is characterised by hard rattling behaviour, particularly during the rapid phases of clutches engaging/disengaging and during the gears synchronisation. Some solutions to attenuate the torsional vibrations, and therefore the rattling behaviour of the unloaded gears in a DCT gearbox, can be analysed by the proposed model to determine, as example, the time duration of the gear shift phase or of the pre-selection phase to the next gear, as well as to identify the optimal lubrication conditions of the gear pairs during the gear shift transients.

Keywords: dual clutch; driveline; vibrations; gear box; gear rattle

Citation: Brancati, R.; Pagano, S.; Rocca, E. Dynamic Behaviour of an Automotive Dual Clutch Transmission during Gear Shift Maneuvers. *Appl. Sci.* **2023**, *13*, 4828. https://doi.org/10.3390/app13084828

Academic Editor: Marco Troncossi

Received: 11 March 2023
Revised: 6 April 2023
Accepted: 8 April 2023
Published: 12 April 2023

1. Introduction

Automated Manual Transmissions (AMTs) represent, in the automotive field, the new frontier of automatic transmissions. An AMT derives from a traditional manual gearbox, being more efficient with respect to actual automatic transmissions which adopt torque converters. AMTs can work both in fully automatic mode and in semi-automatic. When the transmission operates in semi-automatic mode, the gear shifting phases are faster, giving enhaced performance and improving the driving feeling. These types of automated manual transmissions are often equipped with a Dual Clutch Transmission system (DCT) which has the advantage, in addition to the fast gear shifting, of avoiding the interruption of the engine torque [1]. A DCT can be considered in practice as two gear boxes in one, where the drive torque is sorted, through two clutches, between the various gear pairs in the odd or in the even branch. In a DCT the gear shifting can be achieved without engine torque interruption, by applying the torque to one of the two clutches when the other clutch starts to be disengaged. This arrangement permits all the gear shifting without any power interruption from the engine to the driveline. Another advantageous feature offered by this type of transmission is the high mechanical efficiency [2]. The gear shifting is generally actuated by adopting electro-mechanical or electro-hydraulic actuators, moved by a strategic transmission control unit (TCU) [3]. In [4] a DCT for automotive driveline has been analysed, with a focus on the control strategies adopted for the gear shifting manoeuvres.

During the clutch engagement / disengagement manoeuvres in the DCT there are many more gears than in a traditional gearbox that are meshing but unloaded, and so hard gear rattle problems grow, giving rise to Noise, Vibration, and Harshness (NVH) problems [5]. Similarly, the synchronizing transients give rise to severe impacts between the unloaded gears' teeth. Gear rattle is a well-known annoying vibro-acoustic phenomenon afflicting automotive gear boxes. The phenomenon is produced by the repeated impacts and rebounds occurring between the teeth of the low-loaded or unloaded gears due to the torque irregularities of the Internal Combustion (I.C.) engines [6]. Moreover, lightly loaded gears are affected by some gear parameters, such as the circumferential backlash, tooth profile modifications, the temperature, oil quantity between the teeth, and the drag torque, resulting in an annoying rattling noise that makes passengers feel uncomfortable. The theme of the gear rattle has been studied from a theoretical and experimental point of view, adopting various methodologies for non-linear analysis, including some original tools based on the Wavelet analysis or on the Hilbert transform [7,8]. Many remedies can be adopted to reduce the above-mentioned disturbance, such as vibration dampers, dual-mass flywheels, or clutch spring systems. A torsional vibration damper, based on the use of magneto-rheological elastomers, has been recently proposed with positive effects in contrasting the vibroacoustic phenomena of a standard gear box [9]. Another beneficial effect on gear rattle attenuation, reported by some theoretical and experimental analyses, is that exerted by the oil interposed between the unloaded gear teeth [10]. The widespread use of this type of transmission highlights the onset of vibroacoustic phenomena that can compromise comfort inside vehicles. Therefore, the technical problems arising from gear rattle in DCT systems cannot be overlooked. Recently this inconvenience, observed by the car manufacturers, is beginning to be studied in the specific literature [11]. So, the present study aims to focus on this problem which seems to be very annoying, especially during the gear shifting transients. The paper reports a tribo-dynamic model developed to analyse the behaviour of a DCT system of an automotive driveline. The analysis highlights the gear rattle phenomenon arising in the many unloaded gear pairs of these transmissions, during the gear synchronisation transients, taking into account the clutch engagement manoeuvres [12]. The simulations carried out have the purpose of guiding the designers of the DCTs towards the best solutions, thus reducing the whole vibro-acoustic issues.

2. The Driveline with DCT

A DCT system of an automotive driveline can be represented as in Figure 1, where a schematic layout of a gear box with six gear pairs is proposed. A flywheel is driven by an I.C. engine, transmitting its power to the gear box by a Dual Clutch mechanism. The gear box has two primary shafts, one for odd pinion gears and another for even pinion gears. Each primary shaft is connected to a secondary shaft bringing the wheels of the odd and even gear pairs, respectively.

Moreover on each secondary shaft, a final gear wheel (W_{even}/W_{odd}) meshing with the differential wheel (D), is mounted. Figure 1 shows two coaxial primary shafts: the inner shaft, locked to the clutch disk Cl_1, drives the odd gears 1, 3, and 5, while the even gears 2, 4, and 6 are driven by the input outer shaft, connected to the clutch Cl_2. Each input shaft receives, alternately, the engine torque from the flywheel through one of the two independent clutches (Cl_1 and Cl_2), which activates the odd or the even branch of the driveline, as requested by the driver. The resistant torque T_r applied at the final wheel D, represents the reduced load acting on the vehicle while the term I_D represents the inertia of the vehicle reduced at W_D gear wheel.

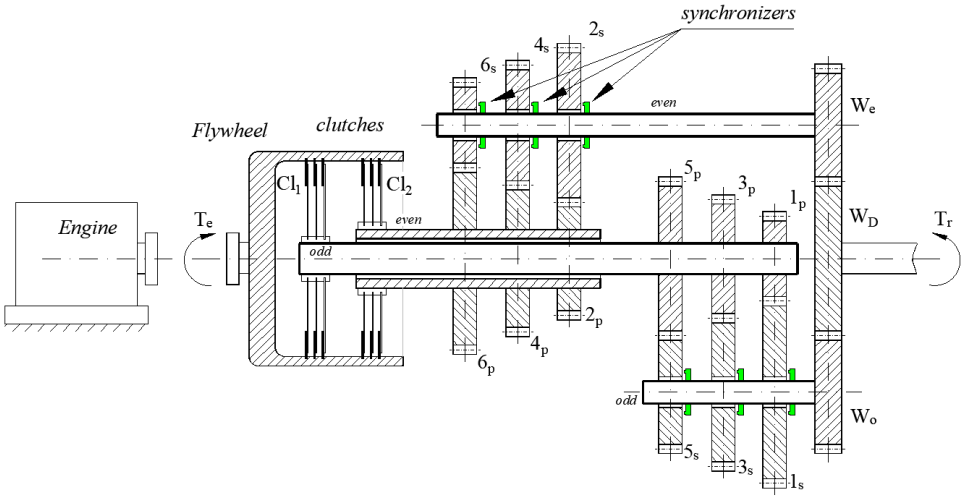

Figure 1. Schematic of a Dual Clutch Transmission system for automotive driveline.

3. The Torsional Model for the Driveline Analysis

The driveline torsional model adopted in the present analysis refers to the physical scheme reported in Figure 1. The model considers the torsional stiffness and damping of the shafts connecting the gear wheels. The gear meshing has been modelled following a theory, adopted for this kind of impacting contacts, considering the squeeze effect of the oil lubricant between the gear teeth. In this way the gear rattle, arising in all the unloaded gears of the gear box, can be highlighted and a deep investigation can be conducted [10]. The phases of clutch operations, as for the gear synchronisation manoeuvres, have been modelled adopting linear functions; in particular, friction forces in the clutches have been modelled adopting the Stribeck hypothesis. The clutch and synchroniser plays a sensitive role for the dynamic behaviour of the transmission and therefore it is important to have an adequate level of theoretical approximation for these components [13–15].

In the following the motion equations for the transmission gear box described in Figure 1 are reported. The transmission gear box has six gear pairs and every gear wheel, comprising the flywheel and the last wheel W_D, is counted in the model. Considering the engine torque T_e and the reduced resisting torque T_r, the motion equations of the flywheel and W_D gear are expressed as:

$$\textbf{Flywheel:} - I_f\ddot{\theta}_f + T_e - T_{cl1} - T_{cl2} = 0 \tag{1}$$

$$\textbf{Gear wheel } W_D\textbf{:} - I_D\ddot{\theta}_D - F_{cD}r_D - T_r = 0 \tag{2}$$

The motion equations for the odd and the even gears, respectively, have been so developed; the equations' parameters are specified in Table 1.

Odd branch (1)

$$\textbf{Clutch 1:} - I_{cl1}\ddot{\theta}_{cl1} - \sigma_{5p}(\dot{\theta}_{cl1} - \dot{\theta}_{5p}) - K_{5p}(\theta_{cl1} - \theta_{5p}) + T_{cl1} = 0 \tag{3}$$

$$\textbf{Gear 1p:} - I_{c1p}\ddot{\theta}_{1p} - \sigma_{13}(\dot{\theta}_{1p} - \dot{\theta}_{3p}) - K_{13}(\theta_{1p} - \theta_{3p}) - F_{c1}r_{1p} = 0 \tag{4}$$

$$\textbf{Gear 1s:} - I_{1s}\ddot{\theta}_{1s} + F_{c1}r_{1s} + F_{sinc\_odd_i} = 0 \tag{5}$$

$$\begin{aligned}\textbf{Gear 3p:} - I_{3p}\ddot{\theta}_{3p} - \sigma_{13}(\dot{\theta}_{3p} - \dot{\theta}_{1p}) - K_{13}(\theta_{3p} - \theta_{1p}) - \\ F_{c3}r_{3p} - \sigma_{35}(\dot{\theta}_{3p} - \dot{\theta}_{5p}) - K_{35}(\theta_{3p} - \theta_{5p}) = 0\end{aligned} \tag{6}$$

$$\textbf{Gear 3s:} - I_{3s}\ddot{\theta}_{3s} + F_{c3}r_{3s} + F_{sinc\_odd_i} = 0 \tag{7}$$

$$\textbf{Gear 5p:} -I_{5p}\ddot{\theta}_{5p} - \sigma_{5p}(\dot{\theta}_{5p} - \dot{\theta}_{cl1}) - K_{5p}(\theta_{5p} - \theta_{cl1}) - F_{c5}r_{5p} - \sigma_{35}(\dot{\theta}_{5p} - \dot{\theta}_{3p}) - K_{35}(\theta_{5p} - \theta_{3p}) = 0 \quad (8)$$

$$\textbf{Gear 5s:} -I_{5s}\ddot{\theta}_{5s} + F_{c5}r_{5s} + F_{sinc\_odd_i} = 0 \quad (9)$$

$$\textbf{Gear } W_0\textbf{:} -I_{W_o}\ddot{\theta}_{W_o} + F_{cD}r_{W_o} - F_{sinc\_odd_i} = 0 \quad (10)$$

$$\textbf{Synchroniser :} F_{sinc\_odd_i} = -\sigma_{iodd}(\dot{\theta}_{is} - \dot{\theta}_{W_o} - K_{iodd}(\theta_{is} - \theta_{W0}) \quad (11)$$

Even branch (2)

$$\textbf{Clutch 2:} -I_{cl2}\ddot{\theta}_{cl2} - \sigma_{6p}(\dot{\theta}_{cl2} - \dot{\theta}_{6p}) - K_2(\theta_{cl2} - \theta_{2p}) + T_{cl2} = 0 \quad (12)$$

$$\textbf{Gear 2p:} -I_{2p}\ddot{\theta}_{2p} - \sigma_{24}(\dot{\theta}_{2p} - \dot{\theta}_{4p}) - K_{24}(\theta_{2p} - \theta_{4p}) - F_{c2}r_{2p} = 0 \quad (13)$$

$$\textbf{Gear 2s:} -I_{2s}\ddot{\theta}_{2s} + F_{c2}r_{2s} + F_{sinc\_even_i} = 0 \quad (14)$$

$$\textbf{Gear 4p:} -I_{4p}\ddot{\theta}_{4p} - \sigma_{24}(\dot{\theta}_{4p} - \dot{\theta}_{2p}) - K_{24}(\theta_{4p} - \theta_{2p}) - F_{c4}r_{4p} - \sigma_{46}(\dot{\theta}_{4p} - \dot{\theta}_{6p}) - K_{46}(\theta_{4p} - \theta_{6p}) = 0 \quad (15)$$

$$\textbf{Gear 4s:} -I_{4s}\ddot{\theta}_{4s} + F_{c4}r_{4s} + F_{sinc\_even_i} = 0 \quad (16)$$

$$\textbf{Gear 6p:} -I_{6p}\ddot{\theta}_{6p} - \sigma_{6p}(\dot{\theta}_{6p} - \dot{\theta}_{cl2}) - K_{6p}(\theta_{6p} - \theta_{cl2}) - F_{c6}r_{6p} - \sigma_{46}(\dot{\theta}_{6p} - \dot{\theta}_{4p}) - K_{46}(\theta_{6p} - \theta_{4p}) = 0 \quad (17)$$

$$\textbf{Gear 6s:} -I_{6s}\ddot{\theta}_{6s} + F_{c6}r_{6s} + F_{sinc\_even_i} = 0 \quad (18)$$

$$\textbf{Gear } W_e\textbf{:} -I_{W_e}\ddot{\theta}_{W_e} + F_{cD}r_{W_e} - F_{sinc\_even_i} = 0 \quad (19)$$

$$\textbf{Synchronisers :} F_{sinc\_even_i} = -\sigma_{even_i}(\dot{\theta}_{is} - \dot{\theta}_{W_e}) - K_{even_i}(\theta_{is} - \theta_{We}) \quad (20)$$

Table 1. Symbols in the motion equations.

Symbol	Description
K_{ij}	Torsional stiffness of the shaft between i-th and j-th pinion gear
K_{5p}	Torsional stiffness of the shaft between Cl_1 and 5th pinion gear
K_{6p}	Torsional stiffness of the shaft between Cl_2 and 6th pinion gear
σ_{ij}	Torsional damping of the shaft between i-th and j-th pinion gear
σ_{5p}	Torsional damping of the shaft between Cl_1 and 5th pinion gear
σ_{6p}	Torsional damping of the shaft between Cl_2 and 6th pinion gear
ω_e	Angular velocity of the engine
ω_v	Angular velocity of the vehicle wheels
I_{ip}	Moment of inertia of the i-th pinion gear (kgm^2)
I_{is}	Moment of inertia of the i-th secondary wheel gear (kgm^2)
θ_{ip}	Angular rotation of the i-th pinion gear (rad/s)
θ_{is}	Angular rotation of the i-th secondary wheel gear (rad/s)
θ_{wo}	Angular rotation of the odd secondary shaft (rad/s)
θ_{we}	Angular rotation of the even secondary shaft (rad/s)
r_{ip}	Pitch radius of the i-th pinion gear
r_{is}	Pitch radius of the i-th secondary wheel gear
F_{ci}	Contact Force exerted between the teeth of the i-th gear

4. The Lubrication Model in the Gear Teeth Contacts

In the present analysis a tribo-dynamic model has been adopted to account for the gear rattle phenomenon generated during the meshing of the gear teeth of all the unloaded gears. The interaction is determined by a force F_{ci} exerted between the tooth flanks of the gears. This force can be due to a direct contact, when the teeth mesh under loading

conditions, or can be due to the oil between the teeth when the tooth flanks of the unloaded gears are approaching before the contacts. F_{ci} forces can be expressed by:

$$F_{ci}(X_i, x_i, \dot{x}_i) = \begin{cases} K(X_i)x_i, & if \quad |x_i \geq b| \\ S(x_i)\dot{x}_i, & if \quad |x_i < b| \end{cases} \tag{21}$$

As regard to the direct force on the correct side of the loaded teeth, the adopted theory is exposed in [16,17]. During the direct contact phase, a nonlinear elastic force applied at the pitch point is considered. This force is obtained using a stiffness function which depends on the position of the pinion gear, and is evaluated by the sum of some terms corresponding to the various tooth pairs contemporarily in contact. For the i-th tooth pair the stiffness term is:

$$K_i(X) = k_p exp\left(C_a \left| \frac{X - \epsilon X_z/2}{1.125\epsilon_\alpha X_z} \right|^3\right) \tag{22}$$

where ϵ and ϵ_α are, respectively, the total and the transverse contact ratio. X_z is the transverse base pitch. The variable $X = r_p\theta_p$ represents the absolute motion of the pinion gear. Consequently, for a complete meshing cycle, X starts from 0 and ends at ϵX_z. Term k_p represents the stiffness value at the pitch point, which depends on the tooth parameters, along with the coefficient C_a.

The lubricated interaction between the unloaded teeth, due to the oil squeeze effect, is developed and detailed in [10]. The force generated by the oil "squeezed" between the teeth of a gear pair, in the instants preceding the impact, has been obtained from the Reynolds equation. The deduced gear rattle model, adopted in this analysis, was experimentally verified in a previous analysis and is based on the following hypothesis that considers even the main properties of the oil lubricant:

1. Only a single tooth pair engaging at the pitch point is assumed.
2. The teeth are considered as rigid bodies with cylindrical shapes and axes parallel to those of the gear wheels. Cylinder 1 represents the tooth of the driving gear, while cylinder 2 represents the tooth of the driven gear wheel.
3. Each cylinder has a radius (r_1 and r_2) equal to the involute radius at the pitch point.
4. The slip velocity of the oil in the lubricated contact between the teeth (along the x direction) is neglected.
5. The oil viscosity is assumed to be constant.

A scheme of the tooth surfaces is then represented in the Figure 2, where, in accordance with the above mentioned hypotheses, the teeth of two wheels are depicted as two cylindrical bodies with radii r_1 and r_2, approaching each other along the η direction:

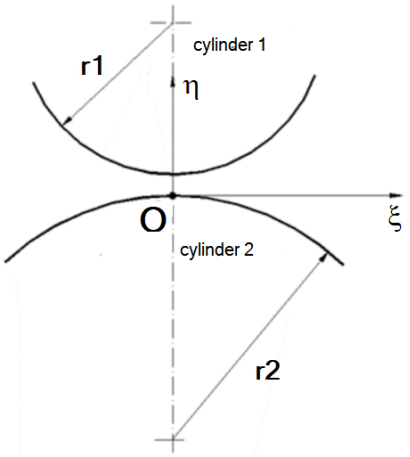

Figure 2. Scheme of the tooth pair contact.

The Reynolds equation, with the above-mentioned hypotheses, can be formulated in the mono-dimensional expression:

$$\frac{1}{\mu}\frac{\partial}{\partial\xi}\left(h^3\frac{\partial p}{\partial\xi}\right) = 12\frac{\partial h}{\partial t} \tag{23}$$

with: p = oil pressure; h = distance between the teeth surfaces; μ = oil dynamic viscosity. The gap height $h(\xi)$ between the teeth can be approximated by the following formula:

$$h(\xi) = h_0 + \frac{1}{2}\xi^2\left(\frac{1}{r_1} + \frac{1}{r_2}\right) \tag{24}$$

with h_0 indicating the minimum distance between the two surfaces.
Assuming:

$$R = 2\left(\frac{r_1 r_2}{r_1 + r_2}\right) \tag{25}$$

the gap is:

$$h(\xi) = h_0 + \frac{\xi^2}{R} \tag{26}$$

Imposing the boundary condition:

$$\begin{cases} \xi = -a \rightarrow p = 0 \\ \xi = 0 \rightarrow \dfrac{\partial p}{\partial\xi} = 0 \end{cases} \tag{27}$$

Integrating the Reynolds equation, the expression of the pressure due to the oil between the teeth can thus be obtained:

$$p(\xi) = 3R^3\mu\left(\frac{1}{(a^2 + Rh_0)^2} - \frac{1}{(\xi^2 + Rh_0)^2}\right) \tag{28}$$

where a represents the semi-length of the oil film along ξ direction, related to the lubrication conditions. By integrating the above relation along the ξ coordinate in the range (−a,a), the analytical expression for the oil squeeze force (21) is obtained:

$$F_c = \dot{x}S(x,a) = -\dot{x}3\mu Z R^{3/2}\frac{[a(a^2 - Rx)\sqrt{Rx} + (a^2 + Rx)^2\arctan(\frac{a}{\sqrt{Rx}})]}{x^{3/2}(a^2 + Rx)^2} \tag{29}$$

In which Z indicates the axial width of the gear pair, $x = \theta_r r_s = (\theta_p - \theta_s)r_s$ and $\dot{x} = \dot{\theta_r} r_s = (\dot{\theta_p} - \dot{\theta_i})r_s$.

In the present numerical analysis all the various gear pairs have been subject to full-meatus lubrication conditions, that is, with oil distributed along the entire tooth flanks. Moreover, the oil lubrication characteristics are those of a typical lubricant for mechanical transmissions with a SAE 75W90 gradation, operating at a low temperature (oil viscosity μ = 0.02 Pa s).

In previous experimental analyses, conducted on a specific test rig at the laboratory of Industrial Engineering Dept. of University "Federico II", designed to carry out investigations on single unloaded gear pairs, the benefit effect of lubricant in reducing the gear rattle phenomenon [10] has been outlined. Figure 3 reports an example of the comparisons between the experimental and theoretical time histories of the angular relative displacement of a gear pair, coming from the automotive gear box corresponding to the 1st gear adopted in the present theoretical analysis, under rattling operative conditions. Geometrical and dimensional parameters of the gear pair are reported in Appendix A (Table A1).

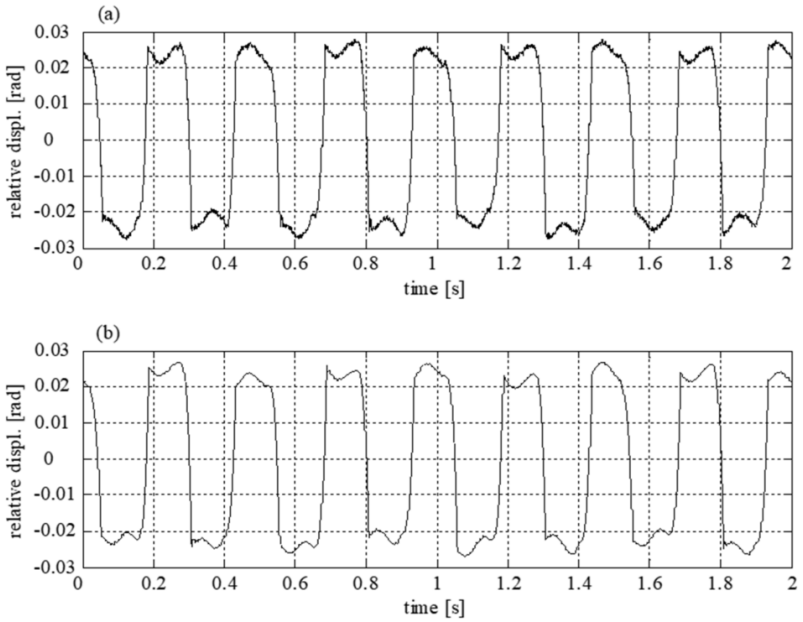

Figure 3. An example of theoretical–experimental correlation for time histories under gear rattle conditions (ω = 600 rpm; $\Delta\omega$ = 100 rpm; f = 4 Hz; (**a**) experimental; (**b**) numerical).

The stationary operative conditions of the test correspond to: speed = 600 rpm; speed fluctuation = 100 rpm; frequency of speed fluctuation = 4 Hz. In this example the gear pair operates under boundary lubrication regime. The good agreement observed in the theoretical-experimental analyses, in the time domain, enables the model to carry out numerical simulations of unloaded gear pairs of automotive gearboxes under rattling conditions, taking into account the effects of lubrication.

5. Clutch Friction Model

Friction in clutches has been modelled following the Stribeck's model. It has been hypothesised that the clutch may be in a stick or slip condition. In the stick phase the clutch transmits the driving torque of the engine T_e, provided that this term is lower than the maximum transmissible torque T_{st} while, during the slip phase, the clutch can transmit a torque value T_{dyn} (dynamic value of the torque) lower than T_e. In the driveline motion equations term T_{cl} can be expressed by [18]:

$$\begin{cases} T_{cl} = min(T_e, T_{st}) & if \left| \dot{\vartheta}_f - \dot{\vartheta}_{cl} \right| < \Delta \\ T_{cl} = T_{dyn} & if \left| \dot{\vartheta}_f - \dot{\vartheta}_{cl} \right| \geq \Delta \end{cases} \tag{30}$$

being:

$$T_{st} = \mu_{st} F_{sp}(t) R_m \tag{31}$$

$$T_{dyn} = \left[\mu_\infty - (\mu_\infty - \mu_0) e^{\frac{\left| \dot{\theta}_f - \dot{\theta}_{cl} \right|}{\alpha}} \right] F_{sp}(t) R_m \tag{32}$$

The clutch spring force F_{sp} is linearly variable from 0 up to a constant value during the clutch engagement phase. Δ is a deviation. R_m is a geometric factor of the clutch given by: $R_m = \frac{2}{3} \frac{R_o^3 - R_i^3}{R_o^2 - R_i^2}$.

The term μ_{st} represents the static value of the friction coefficient; μ_0 and μ_∞ are, respectively, the transition and limit values of the kinetic friction coefficient.

6. The Transients during Gear Shift

Many vibroacoustic phenomena occur during the gear shift transients of this type of transmissions and, as said above, the most relevant is the gear rattle due to numerous unloaded gears. The presence of idle gears is generally greater in a gear box equipped with a DCT than in a conventional automotive transmission fitted with only one clutch. Therefore, in these types of transmissions, the vibroacoustic disturbance can worsen during a gear shifting manoeuvre. In fact, by focusing the attention on this transient, two rapid phases take place: a clutch crossing phase, followed by a phase of pre-selection to the next gear. These phases are accompanied by a series of bilateral impacts on the teeth of the unloaded gear wheels, for one or for both the shafts of the two branches of the DCT system. The following figures clarify the above-mentioned transient phases during a gear shifting from 1st gear speed to the 2nd, with the presence of gears under rattling conditions depicted with blue color. The Figure 4 reports the situation of the 1st running gear speed, where the unloaded gears belonging to the same shaft (3rd and 5th) are showing rattling condition, being quiet all the gears on the even shafts, apart the W_{even} gear. Figure 5 refers to the pre-selection phase of the next gear (synchronisation of the 2nd gear) and, due to the inertia of the even primary shaft, now driven by the W_{even} gear, all the unloaded gears on this shaft (2nd, 4th, and 6th) exhibit bilateral impacts between the gear teeth, adding to the odd gears on the other branch. The present phase seems to be so the worst case for the gear rattle phenomenon referred to the whole gear box.

Furthermore, during the following clutch crossing phase (Figure 6), where contemporary clutch Cl_1 disengages and clutch Cl_2 engages, the rattling behaviour is almost the same as the previous case (Figure 5). The rattling pairs in this case are, in fact, the 3rd and 5th of the odd shaft, and the 4th and 6th of the even. Conversely, as represented in the Figure 7, when the gear shifting has been completed with Cl_2 engaged and the 2nd speed in normal running condition, the presence of unloaded rattling pairs is reduced to the 4th and 6th gears, both belonging to the input shaft of the even gears.

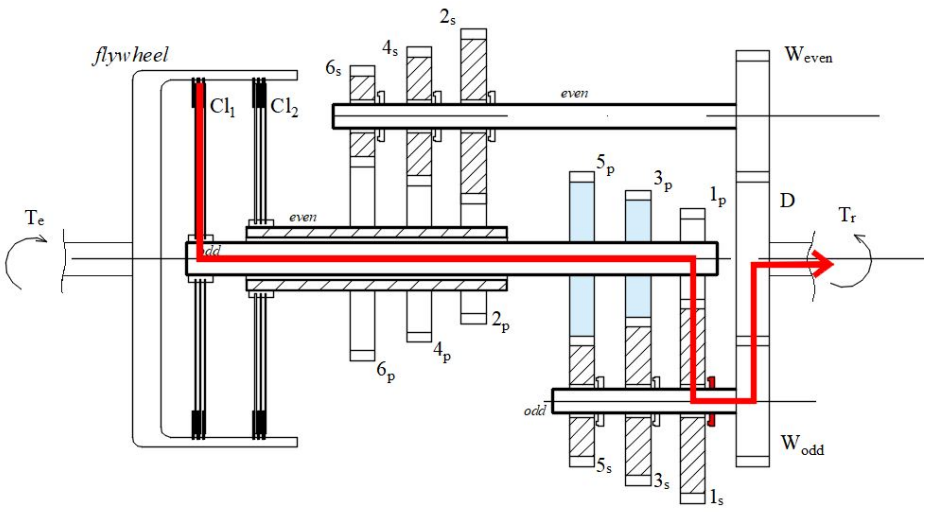

Figure 4. The DCT gear shifting transient: 1st gear synchronised.

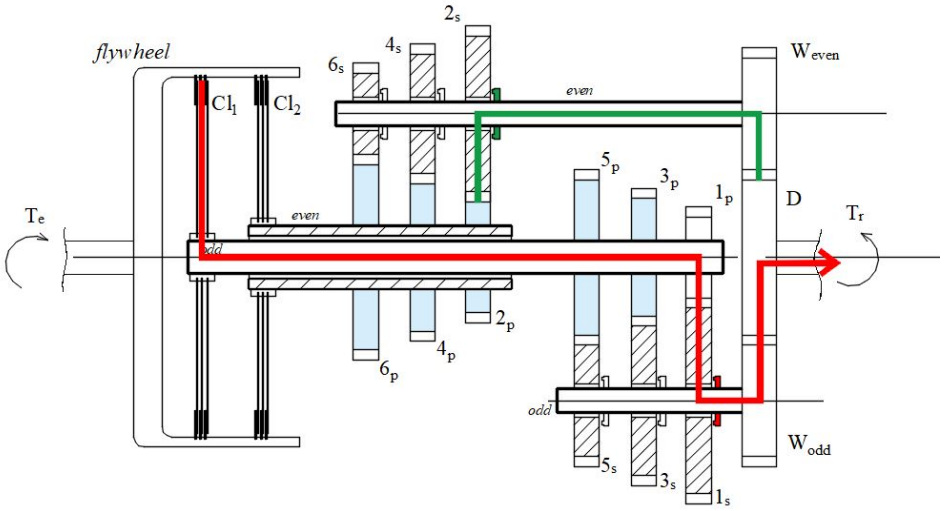

Figure 5. The DCT gear shifting transient: 1st gear running, 2nd gear pre-selected.

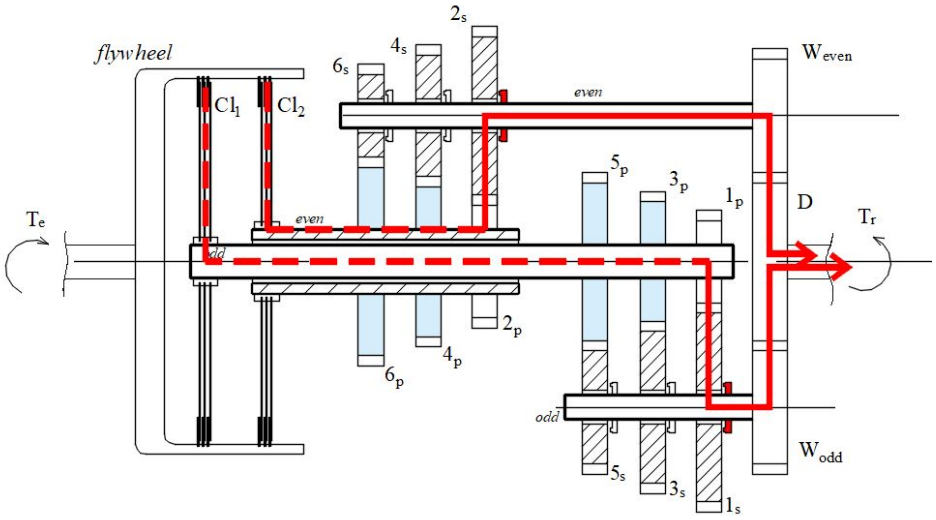

Figure 6. The DCT gear shifting transient: the Cl_1 and Cl_2 clutches crossing phase.

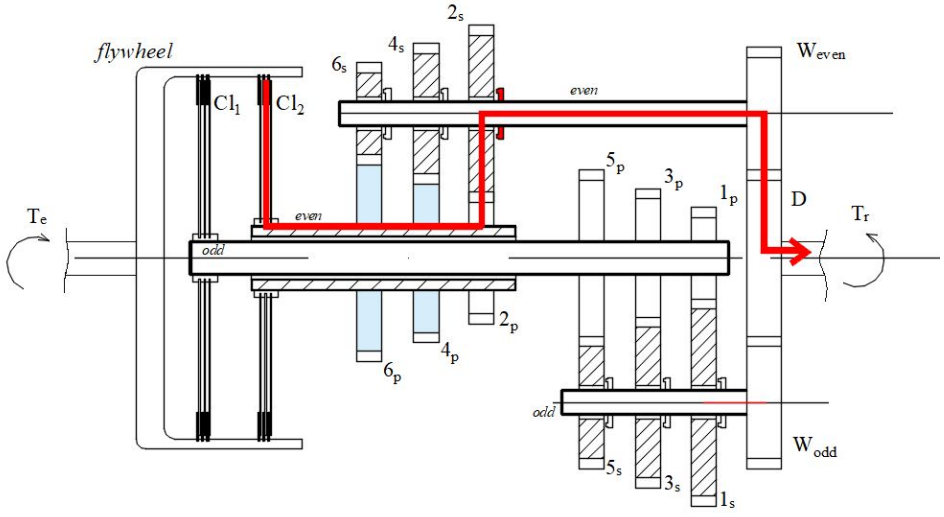

Figure 7. The DCT gear shifting transient: Cl_2 engaged with 2nd gear in running condition.

7. The Results of the Numerical Simulation

The theoretical analysis for a vehicle equipped with a DCT was conducted, referring to values of the inertia parameters reported in Appendix A. The results of the numerical simulations have been analysed by examining the time histories of the shaft angular speed and of the relative angular displacements of the various gear pairs. The gear teeth relative motion examination can be of help to show the qualitative behaviour of the gear pair and so to highlight the severity of the gear rattle phenomenon.

The engine torque law (Figure 8), adopted for the numerical simulations, comes from an actual four-stroke four-cylinder engine and has been obtained from the pressure cycle detected on an experimental test bench. The following Figures 9 and 10 report the time histories of the angular speed for the flywheel and the two clutches during a 10 s run-up transient. In the numerical simulations, the engine speed value is considered equal to 4000 rpm, starting with the 1st speed synchronised. In this instant, the clutch Cl_1 begins to be engaged, while the subsequent gear shifting phases, up to the 4th gear ratio, follow one another with regular time lapse. It must be noted that an oscillation involving a wheel on the unloaded shaft does not affect the oscillations of the wheels placed on the loaded shaft. Two different strategies have been tested:

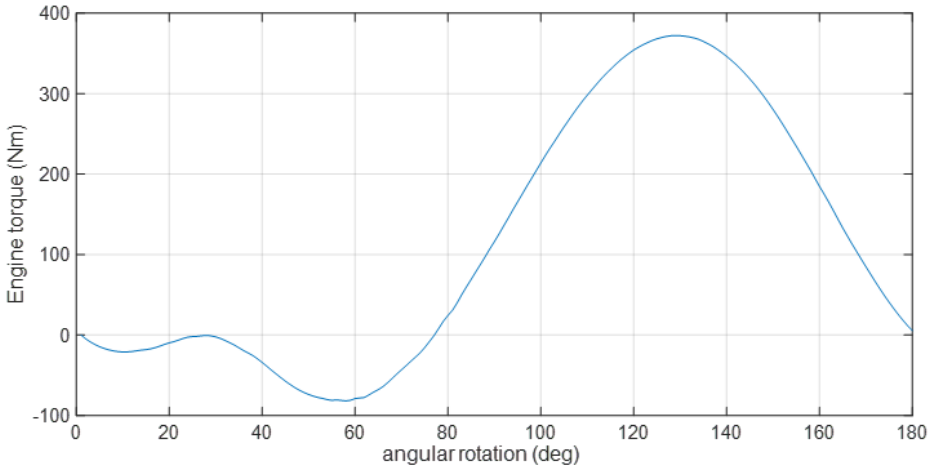

Figure 8. The experimental torque law of the I.C. Engine with four cylinders, four strokes.

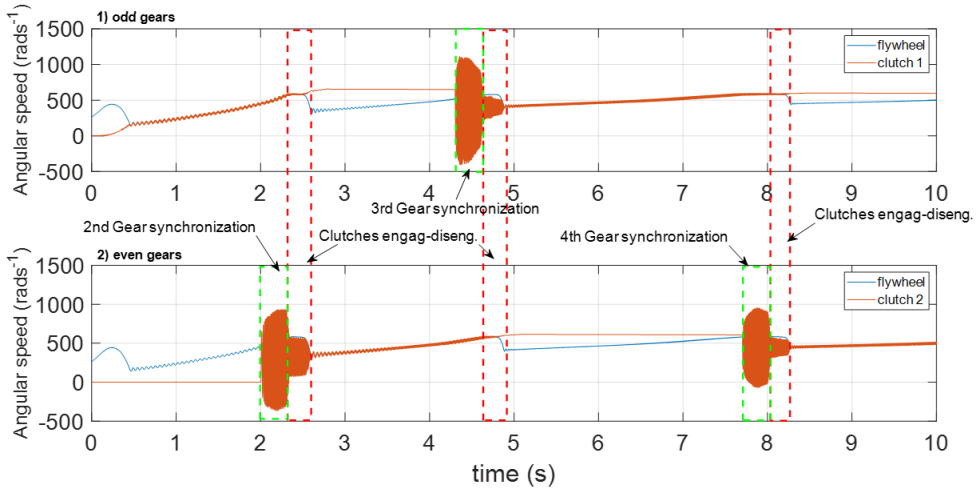

Figure 9. Angular speed of flywheel and clutches during a run-up transient for case (a): (1) odd gears; (2) even gears.

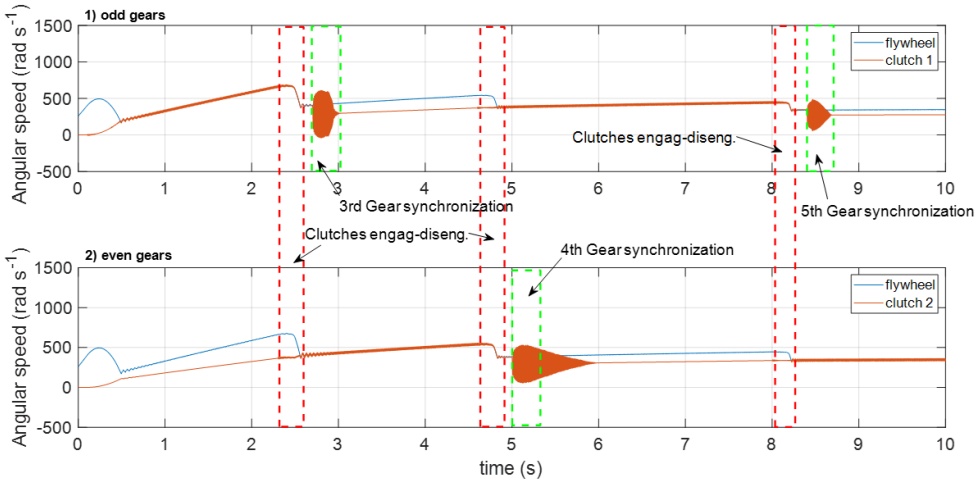

Figure 10. The DCT gear shifting transient: Cl_2 engaged with 2nd gear in running condition.

7.1. First Strategy: ***CASE (a)***

The first one consists in the following steps: initially, the 1st gear is synchronized while all the other gear pairs were synchronized afterwards, just before the upshift manoeuvre. As an example, the 3rd is synchronized after the 2nd speed has finished its running phase. So, every transient of gear shift consists in a rapid gear synchronization followed by a crossing phase between the two clutches.

In the Figure 9 the various phases of the gear synchronisation, together with the engagement/disengagement of the two clutches, are indicated (highlighted with green and red dotted boxes).

The time history, in correspondence with the instant 2 s, shows the 2nd gear which begins the synchronisation process on the even input shaft. On this shaft a sudden increase in the fluctuation amplitude of the gear speed is noted, well evidenced in the green box of the Figure 9, 2. The phase is followed by the engagement of clutch Cl_2 that contributes to reduce the speed fluctuations during this "torque phase". Right after this phase the transmission odd shaft returns to a normal running condition, up to the pre-selection of the 3rd gear (happening around 4.3 s). In this condition, the same behaviour previously observed for the 1st to 2nd shift manoeuvre is reproposed, with great speed fluctuations up to the end of the Cl_1 clutch full engagement on the odd shaft (about 4.9 s). An analogous behaviour is observed when the 4th gear is synchronised (about 7.7 s in the Figure 10) and the engagement transient of clutch 2 takes place (8.1 s). This type of disturbance in the DCT dynamics transient can be ameliorated by modifying the sequence of both the gear shift and clutch operation phases, as given below:

7.2. Second Strategy: ***CASE (b)***

A different strategy was tested which consists of advancing the presynchronisation phase to the next gear as soon as the engagement phase of the clutch in the previous gear speed is completed. For example, 3rd gear is synchronised as soon as 2nd gear has been engaged by clutch 2. Therefore, in the Figure 10 the behaviour of the DCT dynamics obtained following this logic can be observed; the start-up begins engaging the clutch 1 when 1st and 2nd gears are already synchronised on the respective shafts. Hence, when the user wants to switch to the second gear in engagement (approximately 2.3 s), the engagement and disengagement phases of the clutches are not accompanied by large fluctuations in the speed of the two shafts. At this point, as soon as the second gear is running, the pre-selection of the next 3rd gear can be actuated on the odd shaft through the synchronisers. In this case there is also a reduction in the oscillations of the odd shaft gears. The reduction compared to the previous case history is of about 40%. The procedure has been repeated for the various successive gear shifting, always showing a decrease in

the shaft speed oscillations and, therefore, an improvement for the impact phenomena occurring in the tooth contacts of the various unloaded gear pairs.

7.3. Results comparison.

The best result, obtained according to this strategy of advancing the pre-selection phases to the next gears (case b), can be better evaluated by observing Figures 11 and 12, where the gear motion of the various gear pairs are reported. These figures compare the differences in terms of rattling behaviour referring to the above different strategies adopted in the case histories.

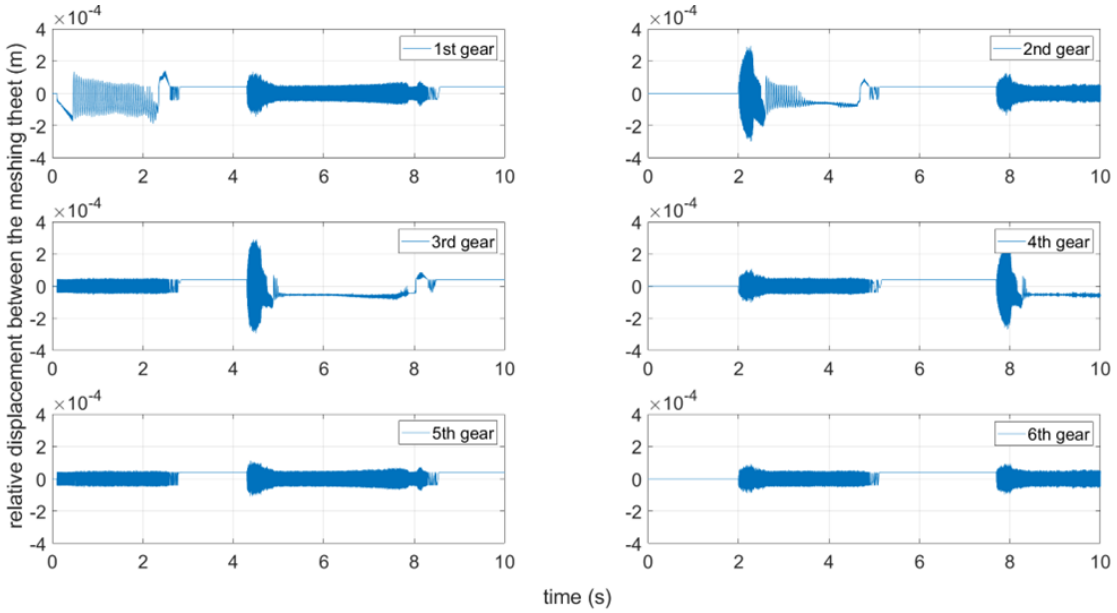

Figure 11. Angular relative motions of the various rattling gear pairs during a run-up transient: case (a).

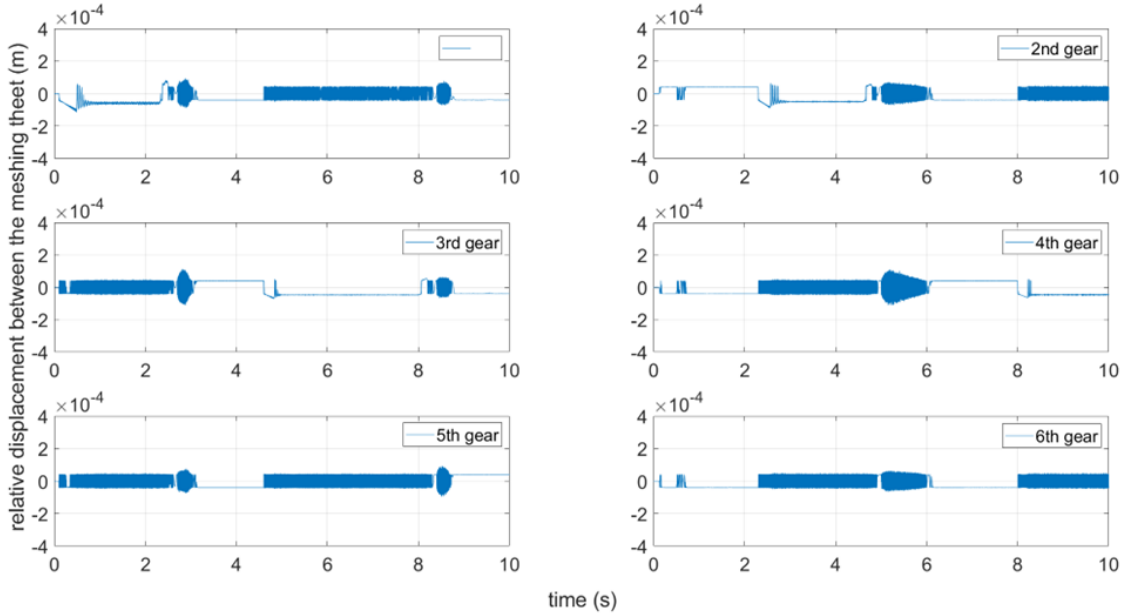

Figure 12. Angular relative motions of the various rattling gear pairs during a run-up transient: case (b).

These figures show, always for a time duration of 10 s, the angular relative motion between the teeth of the six gear pairs during the various shifting transients. As compared

to the previous strategy (case a) an improvement about the rattling behaviour can be highlighted by observing, in the Figure 12, the time intervals where the synchronisation and the engagement and disengagement phases of the clutches occur.

Furthermore, in concomitance with the phases of engagement and disengagement of the clutches, observed in the sequence 1st–2nd (time interval: 2.3–2.6 s in Figure 11); in the sequences 2nd–3rd (4.6 s–4.9 s); 3rd–4th (8.0 s–8.3 s in Figure 12), the relative motion of the gear teeth under load is free from strong deformations. If the teeth relative motion exceeds the circumferential backlash(from -40×10^{-6} m to $+40 \times 10^{-6}$ m) the interaction force is due to direct contact between the loaded teeth, expressed considering the meshing stiffness. This circumstance, evidenced from the comparisons of the results relative to the time histories of both cases of study, highlights better performances for the case b due to a significant reduction in the oscillations of the gear teeth motion. The adopted technique, simulated in the case b, where the gear rattle phenomenon is highly attenuated, represents the correct strategy that can be pursued to improve the vibro-acoustic behaviour of a gearbox equipped with a DCT system.

The better rattling behaviour obtained with the proposed strategy is also confirmed by a frequency analysis. It is well known that for a non-stationary phenomenon the Fourier transform is not useful, but it is necessary to perform a time-frequency analysis. Therefore, the wavelet transform of the 2, 3, 4 gears' angular relative motion has been calculated. Figures 13–15 show diagrams in which the colour indicates the amplitude at a certain frequency and at a certain time instant. By comparison of the second and third gears' angular relative motions wavelet transforms between case (a) and (b) the reduction of vibrations induced is evident. The frequencies of rattle, the yellow lines in the figures, can be obtained multiplying the shaft speed for the gear number of teeth. As an example the rattle frequency of second gear between 2 s and 2.6 s is about 160 Hz (shaft angular speed 500 rpm (8.33 round/s), teeth number 19). For the 4th the improvement is minor, almost negligible.

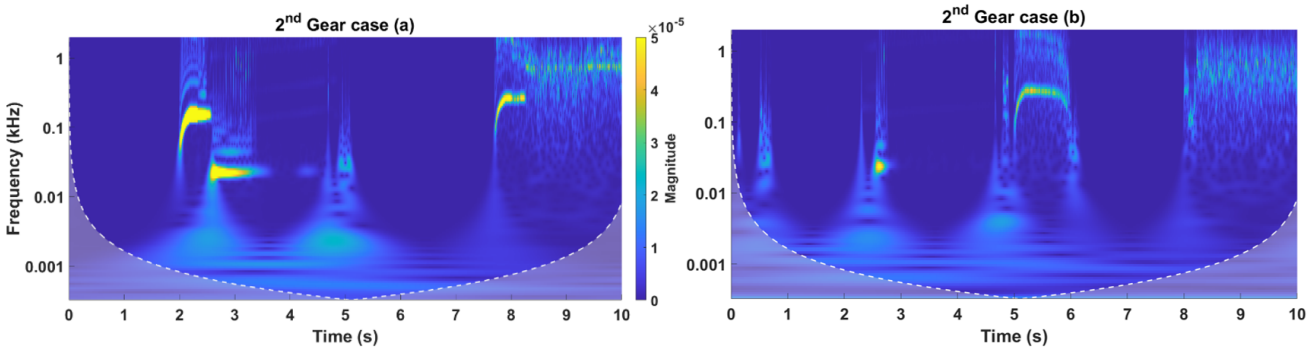

Figure 13. Time-Frequency Wavelet Transform: 2nd gear.

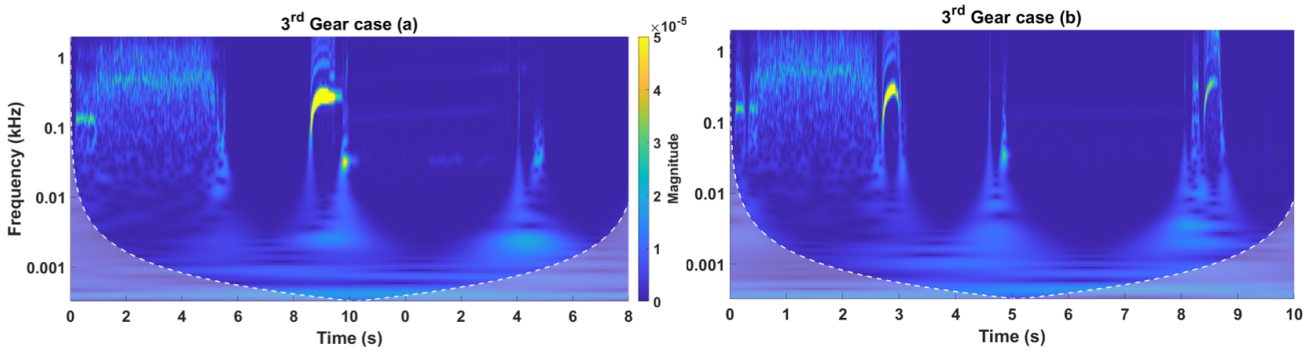

Figure 14. Time-Frequency Wavelet Transform: 3rd gear.

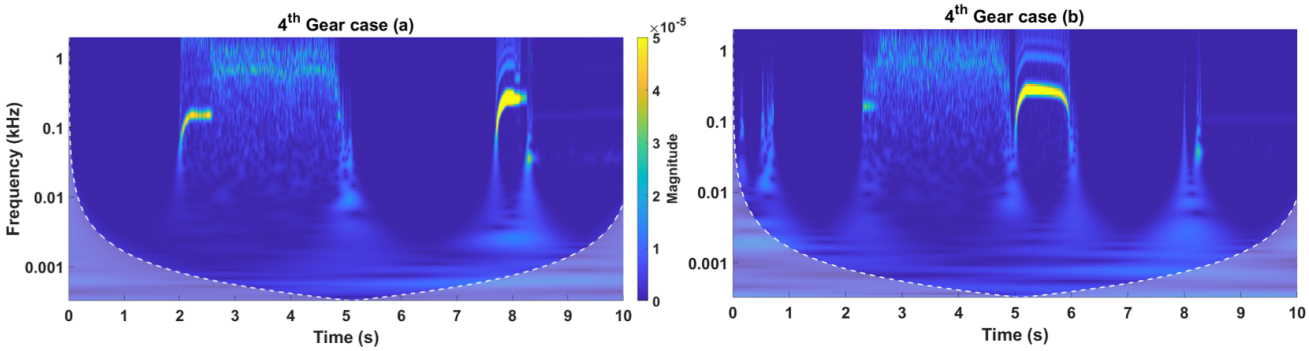

Figure 15. Time-Frequency Wavelet Transform: 4th gear.

8. Conclusions

A model for the dynamic study of the DCT transmissions has been presented that allows the gear rattle phenomenon, particularly felt in the DCT systems due to the high number of non-loaded gear wheels, to be highlighted. The developed model allows NVH problems of the gear boxes that, in the automotive sector, begin to be particularly felt problems, to be analysed and reduced. These algorithms should be combined with those normally adopted to define the gear shift criteria, aiming to optimise driveability and fuel consumption. The developed model considers many factors, such as the phases of engagement and disengagement of the clutch in the gear shift, the synchronisation of the gears, as well as the lubrication between the gear teeth, under some typical simplifying assumptions. The numerical results, obtained adopting this algorithm, have demonstrated that DCT transmission systems are characterised by a strong rattling behaviour, which becomes particularly critical during the rapid phases of the clutch actuations and during the gear pre-synchronisations. The simulations were conducted for different time interval of the engagement and disengagement phases of the two clutches, as well as for the preselection of the gear ratios. The algorithm also allows methods of reducing rattle phenomena to be highlighted. The simulations have shown that an adequate accompaniment of the various manoeuvres and transients allows the annoying vibro-acoustic disturbances of the transmission to be reduced. For example, a positive effect was achieved by anticipating the delicate actuation of the synchronisation to the next gear immediately after disengaging the clutch of the previous gear. To confirm the validity of the results obtained in the time domain, the numerical investigation was supplemented by a wavelet analysis. The theoretical model adopted for the analysis can guide the automotive designers of driveline towards better design strategies, with regard to the many vibro-acoustic issues.

Author Contributions: Conceptualisation, R.B. and E.R.; methodology, E.R. and S.P.; software, E.R.; validation, R.B. and E.R.; formal analysis, R.B. and E.R.; investigation, E.R. and S.P.; writing—original draft preparation, R.B., E.R. and S.P.; writing—review and editing, R.B., E.R. and S.P.; supervision, R.B., E.R. and S.P. All authors have read and agreed to the published version of the manuscript.

Funding: This research received no external funding.

Data Availability Statement: Not applicable.

Acknowledgments: The authors thank Riccardo Russo who has contributed since 2005 to the research on "gear rattle", particularly in the brilliant idea of considering the oil "squeeze effect" between the gear teeth. He also contributed to this paper. His premature death was an irreparable loss to the authors. He will always be fondly remembered.

Conflicts of Interest: The authors declare no conflict of interest.

Abbreviations

The following abbreviations are used in this manuscript:

AMT	Automated Manual Transmissions
DCT	Dual Clutch Transmission
NVH	Noise Vibration Harshness
TCU	Transmission Control Unit
MDPI	Multidisciplinary Digital Publishing Institute
DOAJ	Directory of open access journals
TLA	Three letter acronym
LD	Linear dichroism

Appendix A

The Tables A1–A4 report the numerical values adopted in the simulation.

Table A1. Numerical values of DCT.

Gear	Pinion Numb of Teeth	Pinion Moment of Inertia (kg m^2)	Wheel Numb of Teeth	Wheel Moment of Inertia (kg m^2)	Gear Ratio
I gear	11	1.38×10^{-5}	43	1.36×10^{-3}	3.909091
II gear	19	5.08×10^{-5}	41	8.49×10^{-4}	2.157895
III gear	25	9.67×10^{-5}	37	5.18×10^{-4}	1.480000
IV gear	33	1.66×10^{-4}	37	2.86×10^{-4}	1.121212
V gear	39	2.94×10^{-4}	35	1.87×10^{-4}	0.897436
VI gear	37	5.18×10^{-4}	25	9.67×10^{-5}	0.675676

Table A2. Cluth Hub and Flywheel.

Clutch/Flywheel	Moment of Inertia (kg m^2)
Clutch 1	1.00×10^{-2}
Clutch 2	1.00×10^{-2}
Flywheel	1.00×10^{-1}

Table A3. Gear pairs and lubrication parameters.

Pitch radius of 1st pinion gear	$r_{1p} = 13.24 \times 10^{-3}$ m
Pitch radius of 1st driven gear	$r_{1s} = 51.76 \times 10^{-3}$ m
Pitch radius of 2nd pinion gear	$r_{2p} = 20.58 \times 10^{-3}$ m
Pitch radius of 2nd driven gear	$r_{2s} = 44.42 \times 10^{-3}$ m
Pitch radius of 3rd pinion gear	$r_{3p} = 26.21 \times 10^{-3}$ m
Pitch radius of 3rd driven gear	$r_{3s} = 38.79 \times 10^{-3}$ m
Pitch radius of 4th pinion gear	$r_{4p} = 30.64 \times 10^{-3}$ m
Pitch radius of 4th driven gear	$r_{4s} = 34.35 \times 10^{-3}$ m
Pitch radius of 5th pinion gear	$r_{5p} = 34.26 \times 10^{-3}$ m
Pitch radius of 5th driven gear	$r_{5s} = 30.75 \times 10^{-3}$ m
Pitch radius of 6th pinion gear	$r_{6p} = 38.79 \times 10^{-3}$ m
Pitch radius of 6th driven gear	$r_{6s} = 26.21 \times 10^{-3}$ m
Pitch radius of W_o pinion gear	$r_{Wo} = 34.26 \times 10^{-3}$ m
Pitch radius of W_e driven gear	$r_{We} = 30.75 \times 10^{-3}$ m
Pitch radius of W_D driven gear	$r_{WD} = 30.75 \times 10^{-3}$ m
Half-Circumferential Backlash of gears	b = 40×10^{-6} m
Absolute Oil Viscosity	μ = 0.02 Pas

Table A4. Moment of Inertia.

Vehicle reduced mass moment of inertia	$I_D = 10.0\ \text{kgm}^2$
Moment of Inertia gear W_e	$I_{We} = 1.37 \times 10^{-5}\ \text{kgm}^2$
Moment of Inertia gear W_o	$I_{Wo} = 1.37 \times 10^{-5}\ \text{kgm}^2$

References

1. Senatore, A. Advances in the automotive systems: An overview of dual-clutch transmissions. *Recent Patents Mech. Eng.* **2009**, *2*, 93–101. [CrossRef]
2. Vacca, F.; De Pinto, S.; Hartavi Karci, A.E.; Gruber, P.; Viotto, F.; Cavallino, C.; Rossi, J.; Sorniotti, A. On the Energy Efficiency of Dual Clutch Transmissions and Automated Manual Transmissions. *Energies* **2017**, *10*, 1562. [CrossRef]
3. Bera, P.; Sikora, W.; Wędrychowicz, D. Non-linear control of a gear shift process in a dual-clutch transmission based on a neural engine model. *Control Eng. Pract.* **2021**, *115*, 104886. [CrossRef]
4. Liu, Y.; Qin, D.; Jiang, H.; Zhang, Y. A Systematic Model for Dynamics and Control of Dual Clutch Transmissions. *J. Mech. Des. J. Mech. Design* **2009**, *131*, 061012. [CrossRef]
5. Galvagno, E.; Guercioni, G.R.; Vigliani, A. *Sensitivity Analysis of the Design Parameters of a Dual-Clutch Transmission Focused on NVH Performance*; Technical Report, SAE Technical Paper; SAE International: Warrendale, PA, USA, 2016.
6. Wang, M.Y.; Manoj, R.; Zhao, W. Gear rattle modelling and analysis for automotive manual transmissions. *Proc. Inst. Mech. Eng. Part D J. Automob. Eng.* **2001**, *215*, 241–258. [CrossRef]
7. Brancati, R.; Farroni, F.; Rocca, E.; Savino, S. Analysis of gear rattle by means of a wavelet-based signal processing procedure. *Meccanica* **2012**, *48*, 1399–1413. [CrossRef]
8. Brancati, R.; Rocca, E.; Lauria, D. Feasibility study of the Hilbert transform in detecting the gear rattle phenomenon of automotive transmissions. *J. Vib. Control* **2018**, *24*, 2631–2641. [CrossRef]
9. Brancati, R.; Rocca, E.; Russo, R. Gear rattle reduction in an automotive driveline by the adoption of a flywheel with an innovative torsional vibration damper. *Proc. Inst. Mech. Eng. Part K J. Multi-Body Dyn.* **2019**, *233*, 777–791. [CrossRef]
10. Russo, R.; Brancati, R.; Rocca, E. Experimental investigations about the influence of oil lubricant between teeth on the gear rattle phenomenon. *J. Sound Vib.* **2009**, *321*, 647–661. [CrossRef]
11. Guo, D.; Ning, Q.; Ge, S.; Zhou, Y.; Luo, R. Dynamic Analysis of Gear Rattling of a Certain Type of Dual-Clutch Transmission. *Machines* **2022**, *10*, 805. [CrossRef]
12. Walker, P.D.; Zhang, N.; Zhan, W.; Zhu, B. Modelling and simulation of gear synchronisation and shifting in dual-clutch transmission equipped powertrains. *Proc. Inst. Mech. Eng. Part C J. Mech. Eng. Sci.* **2013**, *227*, 276–287. [CrossRef]
13. Galvagno, E.; Velardocchia, M.; Vigliani, A. Dynamic and kinematic model of a dual clutch transmission. *Mech. Mach. Theory* **2011**, *46*, 794–805. [CrossRef]
14. Walker, P.D.; Zhang, N. Investigation of synchroniser engagement in dual clutch transmission equipped powertrains. *J. Sound Vib.* **2012**, *331*, 1398–1412. [CrossRef]
15. Oh, J.J.; Choi, S.B.; Kim, J. Driveline modeling and estimation of individual clutch torque during gear shifts for dual clutch transmission. *Mechatronics* **2014**, *24*, 449–463. [CrossRef]
16. Cai, Y. Simulation on the rotational vibration of helical gears in consideration of the tooth separation phenomenon (a new stiffness function of helical involute tooth pair). *J. Mech. Des. Sep.* **1995**, *117*, 460–469. [CrossRef]
17. Umezawa, K.; Suzuki, T.; Sato, T. Vibration of power transmission helical gears: Approximate equation of tooth stiffness. *Bull. JSME* **1986**, *29*, 1605–1611. [CrossRef]
18. Duque, E.L.; Barreto, M.A.; de Toledo Fleury, A. Use of different friction models on the automotive clutch energy simulation during vehicle launch. *ABCM Symp. Ser. Mechatron* **2012**, *5*, 1376.